J Am Oil Chem Soc
DOI 10.1007/s11746-016-2896-4

ORIGINAL PAPER

Coalescence Behavior of Pure and Natural Fat Droplets Characterized via Micromanipulation

A. E. Thiel[1] · R. W. Hartel[1] · P. T. Spicer[2] · K. J. Hendrickson[1]

Received: 28 May 2016 / Revised: 8 August 2016 / Accepted: 25 August 2016

Abstract For two approaching oil droplets, a region of arrested coalescence lies between full coalescence and total stability. Here the fusion of two droplets begins, but they are stopped from fully relaxing into one spherical droplet. The internal rigidity of the solid fat network within each droplet can provide the resistance necessary to arrest the shape change driven by Laplace pressure. These intermediate doublet structures lead to the partially-coalesced fat networks important for the desired physical properties of ice cream and whipped topping. The use of micromanipulation techniques allows coalescence events between two oil droplets to be microscopically observed. In this study, oil droplets composed of different fats were manipulated at varying elastic moduli, interfacial tension, and radii. It was seen that increasing the elastic moduli of the droplets or increasing droplet radii resulted in coalescence being arrested earlier. Under these experimental conditions, different interfacial tensions did not change the coalescence behavior between two oil droplets.

Keywords Coalescence · Arrested coalescence · Fat · Emulsion

✉ R. W. Hartel
rwhartel@wisc.edu

[1] Department of Food Science, University of Wisconsin-Madison, 1605 Linden Drive, Madison, WI 53706, USA

[2] School of Chemical Engineering, University of New South Wales, Anzac Parade, Kensington, NSW 2033, Australia

Introduction

Arrested coalescence, sometimes called partial coalescence, is an oil-in-water emulsion destabilization that occurs when the merging of two droplets is initiated, but ceases before total coalescence is reached. This phenomenon results in the formation of intermediate structures and stable doublets with each droplet retaining some of its individual shape [1–5]. Energetically, two droplets would be driven by Laplace pressure to create one larger spherical droplet minimizing the interfacial area. However, the presence of an internal crystalline fat network or interfacial particles coating the surface of droplets can provide an opposing force to arrest coalescence [1, 5–8].

A generally accepted mechanism explaining the occurrence of arrested coalescence was first proposed by van Boekel and Walstra [9]. The hypothesis states that emulsified oil droplets may contain crystalline fat protrusions near the droplet interface that extend into the aqueous phase. As two globules approach each other, the interfacial crystal can pierce through the thin film separating the droplets and enter into the oil phase of the second droplet. If there is enough liquid oil present, an oil neck will be formed around the penetrating fat crystal, as it would prefer to be wetted with oil, rather than the aqueous phase. The oil neck ultimately forms a bridge between the two droplets [1, 3, 9–11]. A key feature of this proposed mechanism is that large, protruding interfacial crystals are needed to induce arrested coalescence. In contrast, recent research has observed arrested coalescence in hexadecane droplets containing wax crystals with no obvious protrusions [7]. Additionally, cryo-TEM images of emulsion droplets composed of hydrogenated palm kernel oil and canola oil revealed a rough surface with small, rounded bumps not the long, sharp-like protrusions proposed in the original mechanism [12].

Published online: 12 September 2016

Typically, emulsion instabilities are minimized in order to extend the shelf life of products. However, in many aerated foods, controlled destabilization through arrested coalescence is desired. Several recent studies have investigated how different conditions such as tempering, application of shear, solid fat content (SFC), fatty acid composition, or different emulsifying agents can influence arrested coalescence in oil-in-water emulsions [13–17]. Here, partially-coalesced fat globules form large networks that provide specific rheological and sensorial properties. The partially-coalesced fat matrix in whipped topping stabilizes the foam structure and confers the product excellent stand-up properties [18–22]. The production of partially-coalesced fat networks in ice cream is critical to obtain a smooth texture, desirable stand-up properties, and dryness when extruding [23–26].

Arrested coalescence is often studied in commercial products, like ice cream and whipped topping, where the partially-coalesced fat globule networks have already been formed. Such methods fail to elucidate exactly how or when two oil droplets are able to undergo arrested coalescence. Through new micromanipulation methods, the entire coalescence process, from the initial contact of two droplets to a stabilized end structure, can be directly observed. This eliminates the need to draw conclusions from preformed networks.

Pawar *et al*. [6] first used micromanipulation techniques to investigate how altering the surface coverage of silica particles on emulsified hexadecane droplets changed coalescence behavior. In a second study hexadecane droplets containing wax crystals at different volume fractions were characterized using micromanipulation [7]. These studies validate the use of micromanipulation methods for investigating emulsions that contain particles either at the oil droplet interface or internally, with the latter being examined in the current work.

From these studies, a model was developed to predict the final degree of coalescence, or strain (ε), of two merging droplets [7]. The model proposes an energy balance of two opposing forces: the interfacial energy and the elastic energy of the internal fat network of the droplets. As two droplets coalesce into one larger droplet, the interfacial energy is decreased as the interfacial area is reduced. This can be offset by the energy needed to rearrange or breakdown the internal fat matrix within each globule during coalescence. Arrested coalescence occurs when the interfacial and elastic energy balance each other at an intermediate state. Total stability or full coalescence will arise when either the elastic energy or interfacial energy dominates, respectively. For two merging droplets, coalescence will be stopped once the lowest energy state is reached.

In this work, the proposed model was tested to fit emulsions containing oil droplets of both high-purity lipids and natural fats. For each fat system, micromanipulation techniques were used to investigate the effect of changing droplet radii and SFC on the degree of coalescence between two droplets. The role of interfacial tension was also explored through varying the concentration of surfactant in pure and natural fat emulsions.

Materials and Methods

Materials

Glyceryl tristearate and glyceryl trioleate of 99 % purity or higher were purchased from Sigma (St. Louis, MO, USA). The anhydrous milk fat fractions were kindly provided by Nutrical (Mexico City, Mexico). Palm oil, palm kernel oil, and coconut stearin were donated by IOI Loders Croklaan (Channahon, IL, USA), AAK (Malmö, Sweden), and Columbus Vegetable Oils (Des Plaines, IL, USA), respectively. The surfactant sodium dodecyl sulfate (SDS) was purchased from Sigma (St. Louis, MO, USA). Methylcellulose was donated by the DOW chemical company (Midland, MI, USA).

Experimental Plan

The first set of experiments involved a high-purity lipid system of tristearin and triolein (Table 1). Micromanipulation was used to investigate the effect of the elastic modulus (G'), interfacial tension (γ), and droplet radius (R), on the extent of coalescence achieved by two droplets. The SFC of the oil phase was changed by altering the ratio of tristearin:triolein, which in turn modified the elastic modulus. Several interfacial tensions were attained by changing the concentration of SDS within the aqueous phase. Different droplet radii could be selected during micromanipulation and droplets within ±10 % of the experimental diameter were deemed acceptable.

A second experiment delved into using natural fats as the oil phase in emulsions. For the anhydrous milk fat (AMF) system, the low-melting fraction was used to dilute

Table 1 Experimental plan for tristearin and triolein system

Variable studied	SDS[a] concentration (mM)	Tristearin in triolein level (wt./wt. %)	Droplet radius (μm)
G'[a]	4	5, 10, 15, 20, and 25	25
γ[a]	0, 2, 4, 8, and 16	15	25
R[a]	4	15	5, 25, 50

[a] *SDS* sodium dodecyl sulfate, G' elastic modulus, γ interfacial tension, R droplet radius

Table 2 Experimental plan for natural lipid systems at different solid fat contents (SFC) including anhydrous milk fat (AMF), palm kernel oil and soybean oil (PKO/SO), palm oil and soybean oil (PO/SO), and coconut stearin and soybean oil (CS/SO)

Fat system	Variable surveyed					
	Elastic modulus (G')			Droplet radius (R)		
	SFC (%)	SDS concentration (mM)	Droplet radius (μm)	SFC (%)	SDS concentration (mM)	Droplet radius (μm)
AMF	4, 6.5, 9, 12, and 15	4	25	9	4	5, 15, 25, 35, 45
PKO/SO	3.5, 5.5, 8, 12, and 18	4	25	8	4	5, 15, 25, 35, 45
PO/SO	3, 7, 9, 11, and 16	4	25	9	4	5, 15, 25, 35, 45
CS/SO	2.5, 4, 5.5, 10, and 30	4	25	5.5	4	5, 15, 25, 35, 45

the high-melting fraction, resulting in a range of SFC. Systems composed of palm kernel oil (PKO), palm oil (PO), or coconut stearin (CS) were paired with soybean oil (SO) to modify the SFC. An experimental design similar to that of the high-purity triglycerides was also applied to the natural lipids systems (Table 2).

For all elastic modulus experiments, each fat system was manipulated at five different SFC. These SFC were specifically chosen since they resulted in droplet pairs arresting in different states of coalescence, as well as total stability and full coalescence during micromanipulation. The elastic modulus of the bulk fat phase was measured for each fat at each SFC. The droplet radius experiments were performed using the middle SFC for each fat. This allowed ample room for the extent of coalescence to increase or decrease as the radius was manipulated.

An interfacial tension experiment was performed using AMF as the lipid phase where the SDS concentration was varied between 2, 4, and 8 mM. A droplet size of 50 μm and an SFC of 9 % was held constant as interfacial tension changed.

Emulsions were made in triplicate for each experimental parameter investigated. Within each emulsion, three droplets pairs were manipulated, yielding nine total pairs per variable.

Emulsion Preparation

Tristearin and Triolein System

The required amounts of tristearin and triolein to formulate a 2 % emulsion were weighed out. Five percent of the tristearin was set aside to be used as a β seed crystal. The fats were transferred into a jacketed beaker that was connected to a waterbath heated to 90 °C. The fats were allowed to melt and then 30 mL of the surfactant solution was added and fats were emulsified for 5 min. Then 1.5 g of methylcellulose was added to the emulsion and agitated for 5 min. The water bath was cooled to 68 °C over the next 25–30 min. Once the water bath reached 68 °C, the tristearin β seeds were added. The emulsion was then transferred from the jacketed beaker into the beaker holding 67 mL surfactant solution at 0–2 °C for quick cooling. Emulsions were held at 4 °C during storage but equilibrated back to room temperature before micromanipulation. At least 12 h was allowed between emulsion preparation and micromanipulation to ensure that fat crystallization had ceased.

Natural Fat Systems

The required amounts of the high-melting and low-melting fats to produce a 2 % emulsion were placed inside a jacketed beaker attached to a waterbath heated to 50 °C. The fat was melted and then 30 mL of the surfactant solution was mixed in for 5 min. Next, 1.5 g methylcellulose was added and stirred in for 5 min. The water bath was then set to cool to 35 °C over 15 min (1.04 °C/min). During this time 67 mL of the surfactant solution was poured into a separate beaker and cooled to 10 °C. Once the water bath reached 35 °C, the emulsion was quickly transferred to the beaker containing the 10 °C surfactant for rapid cooling. Emulsions were stored at room temperature for at least 12 h before micromanipulation.

Solid Fat Content

The Bruker Minispec (Billerica, MA, USA) TD-NMR determined the SFC of all bulk fat samples at room temperature. The desired fats were weighed into NMR tubes and conditioned following the same method the emulsions underwent. Each sample was prepared in triplicate. The SFC was tracked for 48 h to ensure that fat crystallization had concluded. No change in SFC was seen after 12 h.

Interfacial Tension

The pendant drop method on the ThetaLite optical tensiometer (Biolin Scientific, Västra Frölunda, Sweden) measured the interfacial tension between the oil and water phases used in each emulsion. The low-melting fat of the lipid

phase, either triolein, the low-melting fraction of AMF, or soybean oil was placed in a cuvette. A syringe containing the aqueous phase of the emulsion, 1.5 % methylcellulose with the desired concentration of SDS, was used to inject a droplet into the oil-filled cuvette. The tensiometer was equipped with OneAttension software that could record real-time measurements of interfacial tensions using the Young–Laplace equation. Interfacial tension was measured in triplicate for each system.

Rheology

Tristearin and Triolein System

The elastic modulus of the tristearin/triolein fat networks was measured using the Anton-Paar Physica MCR 301 small angle oscillatory rheometer with the concentric cylinder geometry (Graz, Austria). Tristearin and triolein were weighed in the cylinder attachment with 5 % of the tristearin put aside to use as seed crystal. The concentric cylinder attachment was then fixed to the rheometer. The rheometer was heated to 90 °C to melt the fat for 10 min. The spindle was lowered and allowed to equilibrate with the sample for 10 min. The temperature was then cooled to 68 °C. Here the tristearin seed crystals were added and the sample experienced a shear of 60 s^{-1} for 500 s. The temperature was then further reduced to 22 °C and the sample was held for 3 h. After the sample was conditioned, it experienced a shear ramp from 1.0 × 10^{-5} to 10 % at a frequency of 1 Hz. All measurements were taken in triplicate.

Natural Fat Systems

The TA Instruments Discovery HR-2 Hybrid Rheometer (New Castle, DE, USA) was used with the 20-mm parallel plate geometry to quantify the elastic modulus of the natural fat systems. Each fat sample was conditioned in the water bath to mimic the emulsion preparation method above. The rheometer was set to 10 °C to imitate the rapid quenching of the emulsion. The fat was transferred from the water bath and pipetted onto the Peltier plate. The parallel plate was lowered to a gap of 200 μm. The sample was conditioned on the rheometer at 10 °C for 300 s. The temperature was then raised to 25 °C and the sample allowed to equilibrate for 300 s before the oscillation test began. The hour-long test was performed at 25 °C with a frequency of 1 Hz and strain of 0.2 %. All measurements were taken in triplicate.

Micromanipulation

The micromanipulation apparatus was composed of a Nikon Eclipse FN1 microscope (Melville, NY, USA) and a Nikon DS-Fi2 camera in combination with Sutter Instruments (Novato, CA, USA) Xenoworks digital microinjection system. Emulsions were transferred into a glass Petri dish that could be set on the microscope stage. Two pipette tips were fabricated and connected to the Sutter MPC-200 multi-manipulator controller. The two pipettes were lowered into the emulsion followed by the 20× immersion lens. The microinjection unit allows slight suction to be applied through the manipulators to select droplets to be slowly drawn to the pipette tips. The two manipulators were able to move in the *X*, *Y*, and *Z* directions via the Sutter MPC-200 unit. Once two droplets were selected and located at the tip of the manipulators, they could be gently brought into contact to allow coalescence. All events could be watched in real-time through the Nikon NIS Elements software.

Micromanipulator tips were produced from fire-polished borosilicate glass capillary tubes (10 cm length, 1 mm OD and 0.5 mm ID) from Sutter Instruments. Pipette tips were pulled using the P-30 Micropipette Puller from Sutter Instruments. The tip of each pipette was then scored and severed to create a small opening at the end of each capillary tube. The size of the opening of the pipettes was changed as droplets size became larger or smaller.

The coalescence, or lack thereof, between two droplets was recorded as strain (ε), which is defined as:

$$\varepsilon = 1 - [L_T/(L_1 + L_2)], \tag{1}$$

where L_T is the total length of the final coalesced structure. L_1 and L_2 are the diameters of the two original droplets. Here the maximum strain occurring between two droplets is 0.37 or total coalescence, while a strain of zero corresponds to total stability. Any intermediate values of strain relate to the many stages of arrested coalescence.

Mathematical Model Testing

A model to predict the strain between two droplets has been proposed by Pawar *et al*. [7] Eq. (2) accounts for the experimental droplet radius (R), interfacial tension (γ), and elastic modulus (G') of the crystalline fat matrix to predict coalescence behavior.

$$\gamma = (A_2/A_1) \exp(\varepsilon_{min}/A_2) G' R \varepsilon_{min}. \tag{2}$$

Here, ε_{min} is the predicted strain that two droplets will undergo with the experimental conditions inserted into the model. The decay coefficients A_1 and A_2 refer to the changing interfacial area as droplets are coalescing and are assigned values of 0.23 and 0.19, respectively [7]. The model can be rearranged so that both strain values are in the same term:

$$\exp\left(\varepsilon_{min}/A_2\right)\varepsilon_{min} - [(\gamma A_1)/\left(G' R A_2\right)] = 0. \tag{3}$$

For each set of experiments, the interfacial tension, elastic modulus, and droplet radius were entered into the equation and the goal seek function in Microsoft Excel was used to solve for ε_{min}.

Statistics

Statistical analysis was done on JMP Pro 11 using the matched pairs function. Experimental and model strains were compared using two tailed, paired t tests with an $\alpha = 0.05$.

Results and Discussion

For all lipid systems, the changes in coalescence behavior with different droplet diameters and elastic moduli of the internal fat network were investigated. An interfacial tension experiment was performed on both the tristearin/triolein and AMF system.

The energy balance model proposed by Pawar *et al*. [7] was used to obtain predicted strains between two droplets. For each micromanipulation experiment the corresponding droplet radius, interfacial tension, and elastic modulus were inserted into the model equation. This allowed the model strains from the energy balance to be compared to experimental strains from micromanipulation.

Coalescence Images and Mechanism

Each of the five lipid systems was formulated to five different SFC selected to show varying degrees of coalescence between two droplets. For the tristearin and triolein system, the final structure of two droplets put into contact at each SFC is pictured in Fig. 1. At 5 % SFC, two droplets have coalesced to form a larger, almost spherical droplet. Total stability against coalescence is seen at 25 % SFC, where the two oil droplets retain their original structure and share no oil. The three intermediate SFC show different states of arrested coalescence from an ellipsoidal structure to sharing only an oil neck. By measuring the linear deformation of droplet pairs, the effect of the elastic modulus of the crystalline fat network on strain, could be quantified.

The same procedure was repeated for the four natural lipid systems with each prepared to five different SFC. Pictures from the CS/SO system are shown in Fig. 2 to represent the final structures seen using all of the natural fats. It was observed that similar structures could be obtained in both the high-purity and natural fat systems. In both systems, no interfacial crystals can be seen emerging from the droplets.

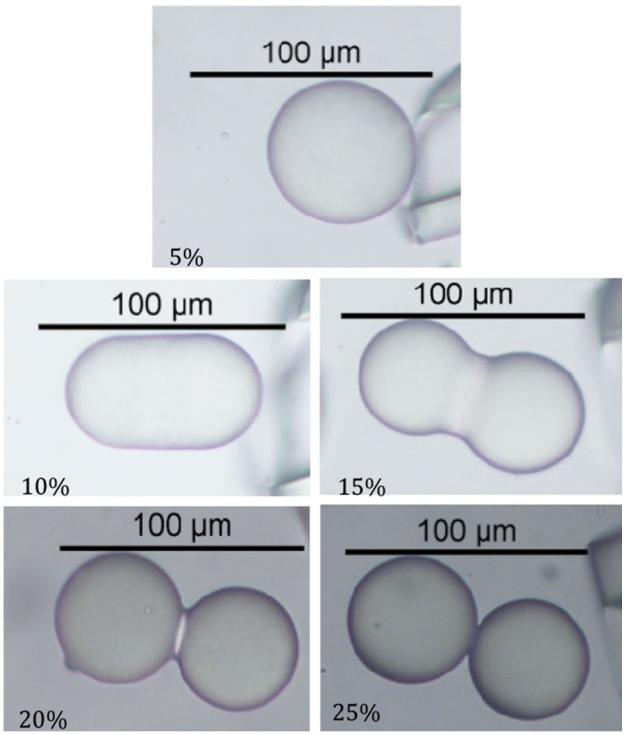

Fig. 1 Final structures observed between two tristearin/triolein droplets formulated to 5, 10, 15, 20 and 25 % solid fat

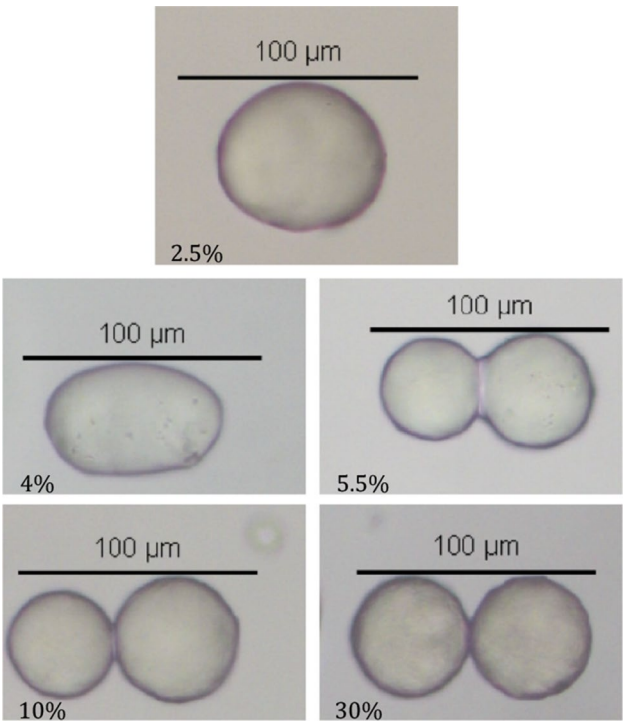

Fig. 2 Final structures observed between two coconut stearin and soybean oil (CS/SO) droplets formulated to 2.5, 4, 5.5, 10, and 30 % solid fat

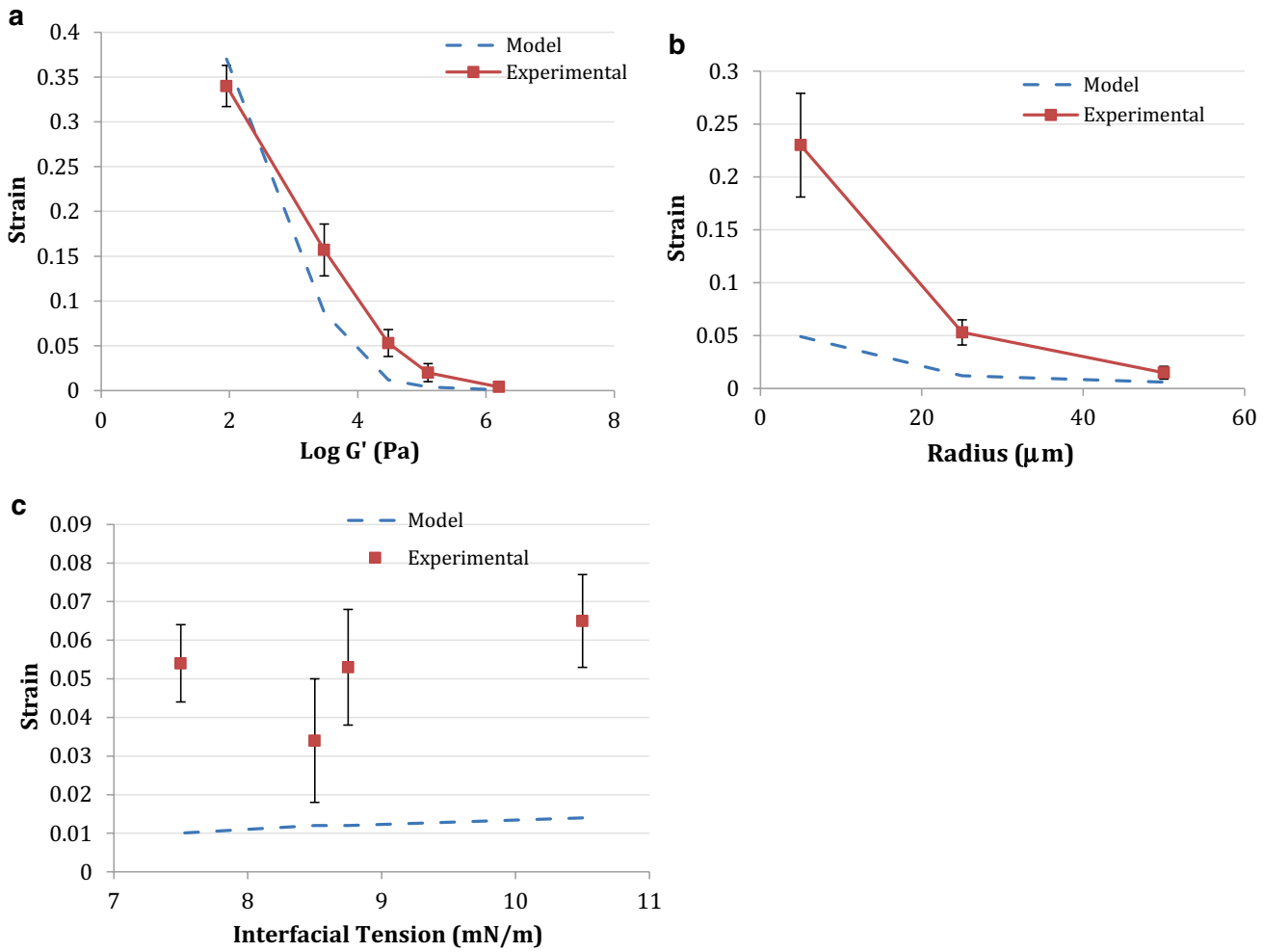

Fig. 3 Experimental and model strain values for tristearin/triolein droplets at **a** five different elastic moduli **b** three different radii **c** four different interfacial tensions

Model Fitting

Tristearin and Triolein System

In this system, the amount of tristearin was continuously increased to yield higher SFC, which results in higher elastic moduli. In Fig. 3a, it is seen that as the elastic modulus increases (with increased SFC), the strain between a pair of droplets decreases. In other words, as the crystalline fat within an oil droplet produces a stronger network, coalescence becomes arrested earlier, until total stability is reached with a SFC of 25 %. This trend is explained by the model, which asserts that as the elastic energy of the crystalline fat matrix is increased, a larger force is needed to deform that network as globules change shape during coalescence.

From rheological testing, the elastic modulus obtained in the linear viscoelastic region for each SFC was used to make model projections. An interfacial tension of 8.40 mN/m and droplets with 25 µm radii were used. In Fig. 3a, the model predicts the same trend seen experimentally for the five different elastic moduli investigated. The model and experimental strains are statistically similar only at the highest log G' where total stability is observed. Compared to some of the natural fats seen in subsequent sections, the model qualitatively follows with the strain observed experimentally in the tristearin/triolein system.

According to the model, full coalescence takes place with a strain of 0.37 where droplets merge to form one spherical globule. In the tristearin and triolein system, a maximum strain of ~0.34 was achieved with emulsions formulated to 5 % SFC. A similar observation was seen in the natural fat systems. Pawar *et al*. [7] observed that for a system of wax and hexadecane, full coalescence took place when droplets approached a strain of 0.34. Here, the coalesced structure retains a slightly oblong shape,

illustrated in Figs. 1 and 2 for 5 % SFC tristearin/triolein and 2.5 % SFC CS/SO, respectively. The tendency of droplets to not fully coalesce into a spherical shape may be explained by the viscous aqueous phase obstructing the shape change and making full coalescence a time-dependent process.

In this high-purity lipid system, three different oil droplet radii 5, 25, and 50 μm, were chosen during micromanipulation to determine the effect of droplet size on coalescence. All emulsions were formulated to 15 % SFC and interfacial tension was held at 8.40 mN/m. Figure 3b shows that increasing the droplet diameter resulted in decreased coalescence for every droplet size. Such observations may be due to smaller droplets having higher curvature and internal pressures. Therefore, the coalescence of two small droplets would be more advantageous than droplets of a larger size.

Comparison of the experimental and model strain values of tristearin/triolein oil droplets of different sizes is seen in Fig. 3b. At a droplet radius of 5 μm, the model largely underestimates the strain seen experimentally. At the two larger droplet radii, the model still underestimates strain but to a lesser degree. It appears that the model can more accurately predict strain as droplet size increased. At all droplet sizes the experimental and model strain were statistically different. The large difference between the model and experimental strain at the smallest radii might be attributed to the 5 μm droplets having a lower SFC than predicted by the bulk measurement or variations in the structure of the internal crystalline network.

By preparing emulsions with different concentrations of the surfactant, SDS, coalescence could be observed between pairs of droplets at several interfacial tensions. It is energetically favorable for two droplets to merge at high interfacial tensions in order to minimize the total interfacial area. At lower interfacial tensions, this advantageous energetic transition diminishes. Therefore, the model predicts that the strain between two droplets would decrease as the interfacial tension was gradually reduced. Figure 3c displays the interfacial tension of 2, 4, 8, and 16 mM SDS with 1.5 % methylcellulose added, and the resultant strain between two droplets. The data point of 0 mM SDS was deleted as excessive force was needed for droplets to coalesce. In this case, the location where the oil droplets were in contact with the micromanipulators led to indentations and alteration of the crystalline fat network.

The model expects a clear trend of higher strain values as interfacial tension is increased; however, this was not seen experimentally. As the SDS concentration was varied from 2 to 16 mM, no obvious change in strain was recorded. Visually, the final coalesced structures at all four interfacial tensions appeared similar. The lack of a trend may be explained by the small range of interfacial tensions achieved even over the wide range of SDS concentrations being used.

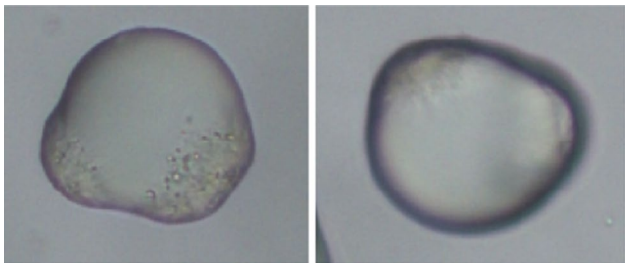

Fig. 4 Example of atypical shape relaxation seen in AMF droplets at 4 % SFC

Initially, methylcellulose was added to thicken the emulsion, but it also has some surface activity. The interfacial tension of pure water in triolein compared to a 1.5 % methylcellulose solution in triolein was 32.25 and 15.13 mN/m, respectively. The presence of methylcellulose in the emulsion, even without any SDS, drastically reduced interfacial tension. Therefore, in the prepared emulsions both SDS and methylcellulose served as surface-active agents. The addition of methylcellulose, solely to ease the process of micromanipulation, resulted in a limited range of interfacial tensions being attained.

Anhydrous Milk Fat System

The first natural fat system was composed of two fractions of AMF. Adding different amounts of the high-melting or low-melting fraction allowed the SFC and elastic modulus to be varied. Originally, five different SFC were tested; however, the 4 % SFC pairs did not relax into a single spherically-shaped droplet as expected. Instead, the coalesced structures had discrete, highly crystalline areas that were pushed to the edge as two droplets merged. This resulted in irregular shapes as pictured in Fig. 4. The 4 % SFC data point was not included since L_T differed depending where the measurement was taken.

The experimental and model strains for the four different elastic moduli achieved are compared in Fig. 5a. Droplets had a radius of 25 μm and interfacial tension was measured at 6.76 mN/m. Again, it was seen that strain became smaller as the internal elasticity of droplets grew stronger. However, the model does not accurately describe the strain values attained by the AMF droplets during micromanipulation. Model projections expect the strain to be lower than observed experimentally, nearly zero at all elastic moduli. This discrepancy may be due to the rheological tests being performed on the bulk fats, while coalescence is observed between two emulsified droplets. The nucleation, crystallization rate, and crystalline network may differ between the

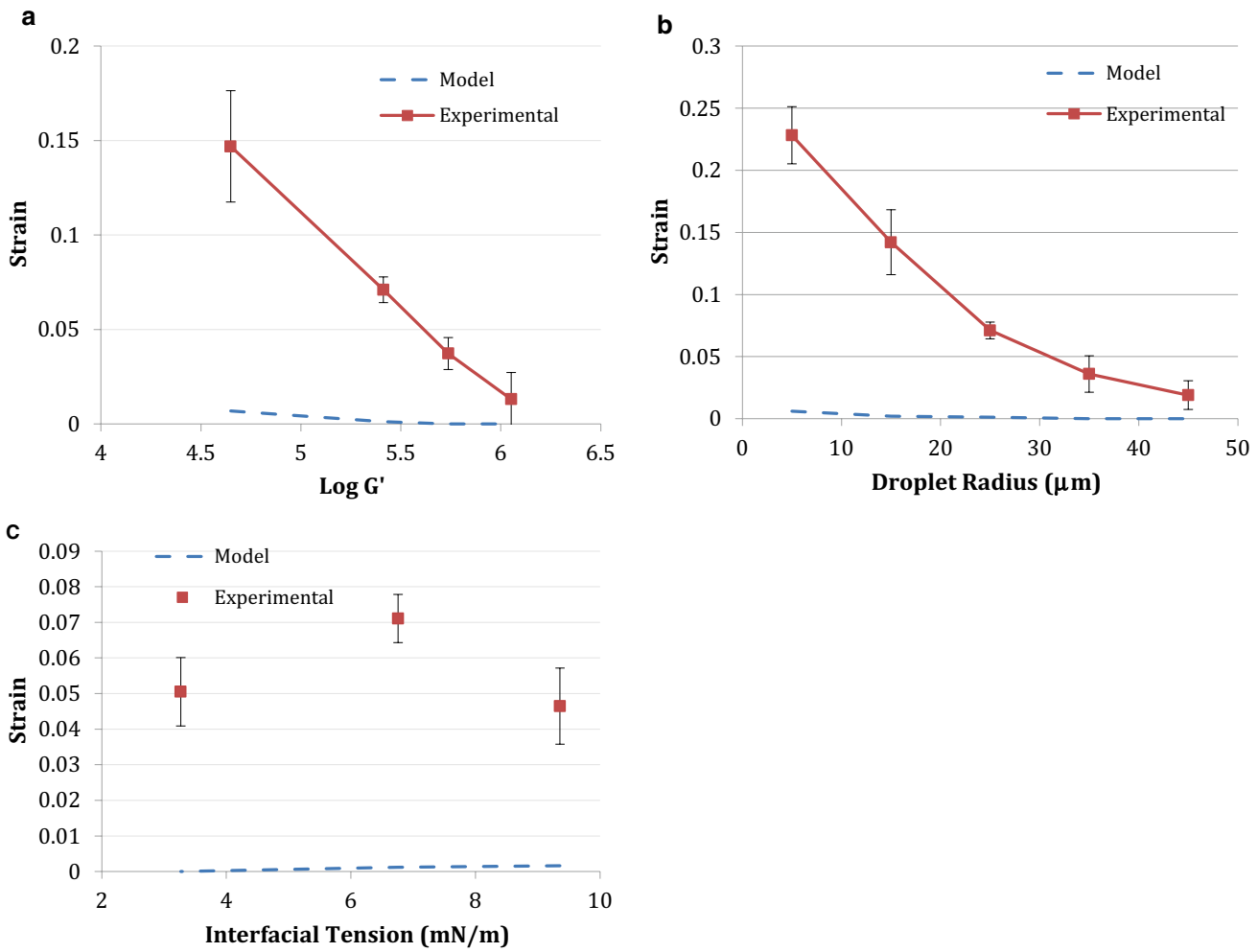

Fig. 5 Experimental and model strain values for anhydrous milk fat (AMF) droplets at **a** four different elastic moduli **b** five different droplet radii **c** three different interfacial tensions

bulk and emulsified fat lending to the differences seen in Fig. 5a. Additionally, AMF is no longer a pure fat system but rather a complex mix of many triglycerides and minor lipid components.

For all natural fat systems, five different droplet radii were micromanipulated, ranging from 5 to 45 µm. For the AMF emulsions, a surface tension of 6.76 mN/m and SFC of 9 % was held constant. It was seen that as droplet radius decreased, there was an increase in coalescence (Fig. 5b) as smaller droplets experienced higher internal pressures. Such results are comparable to the trend seen in the droplet radius experiment using tristearin/triolein.

At all droplet radii investigated, the model projections are significantly lower than the strains seen experimentally. A similar result was seen in the AMF elastic modulus experiment where the model expects a very small range of strain to be observed. Again, the contrasting experimental and model strains might be attributed to differences in the elastic modulus of the bulk versus emulsified fats. Nonetheless, the model appears to be unable to correctly estimate the strain between the AMF droplets under the experimental conditions.

A second interfacial tension experiment was performed using AMF as the lipid phase. Here three different surfactant concentrations of 2, 4, and 8 mM SDS were used, but only a small range of interfacial tensions, 3.27–9.36 mN/m, was achieved. Once again, such low interfacial tensions are attributed to the surface activity of SDS, methylcellulose, and the minor lipids in AMF. Experimentally, no clear trend explaining the relationship between strain and interfacial tension is visible as illustrated in Fig. 5c.

The model predicts lower strains than experimentally observed, nearly zero, for all interfacial tensions tested for the AMF system. This is not surprising as a similar trend was seen for AMF in both the elastic modulus and droplet

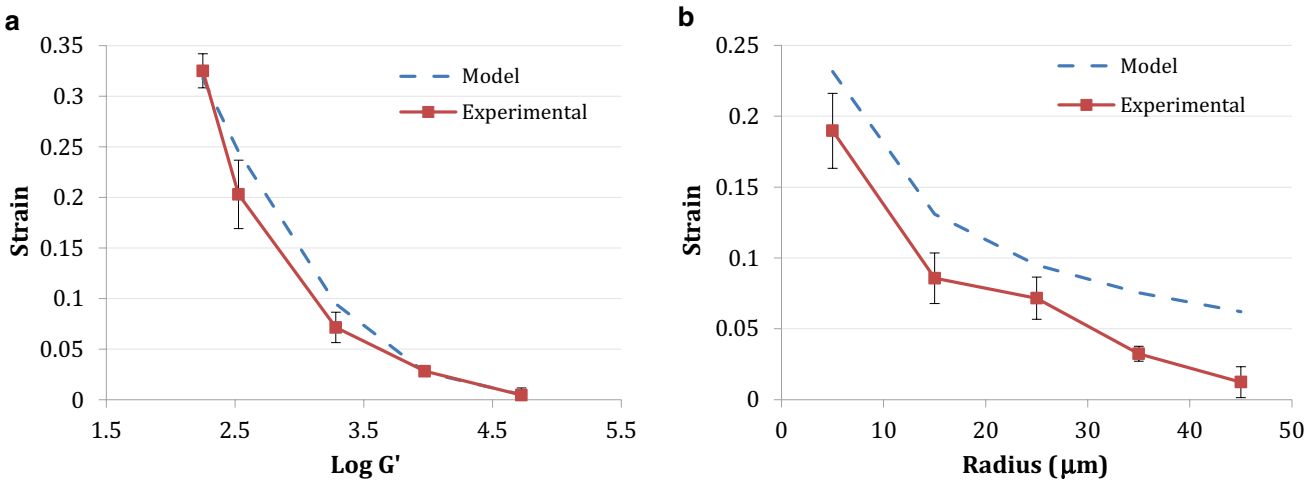

Fig. 6 Experimental and model strain values for palm kernel oil and soybean oil (PKO/SO) droplets at **a** five different elastic moduli **b** five different radii

radius experiments. With this lipid system, the model consistently underestimates the strain between two droplets for all experimental parameters.

The discrepancies between model and experimental strains for AMF might be explained by the large elastic moduli attained by the system. Compared to the other natural fat systems, AMF had the highest elastic modulus values, even at low SFC, the model does not expect two droplets to undergo high degrees of coalescence. The AMF bulk fat that underwent rheological testing does not appear to correctly describe the microstructure of the crystalline fat within emulsified droplets in the way that the model expects.

Palm Kernel Oil and Soybean Oil System

The second natural fat system was composed of palm kernel oil and soybean oil. Again the lipid phase was formulated to five different SFC, the corresponding elastic modulus was found, and the coalescence behavior between two droplets was observed. Figure 6a shows the experimental and model strains for PKO/SO. The model appropriately predicts strain values comparable to the experimental results. Results from the *t* tests confirm that 3.5, 12, and 18 % SFC conditions led to statistically similar experimental and model strains.

Similar to the AMF droplet radii experiment, different droplet sizes were also investigated with the PKO/SO system. Again droplets with radii of 5, 15, 25, 35, and 45 μm were manipulated at a constant interfacial tension of 6.23 mN/m and 8 % SFC. Figure 6b shows the model over predicts the strain seen at each droplet radius. Compared to the results for the AMF system, the model appears to correlate more strongly to the PKO/SO; however, the model and experimental strains are not statistically similar.

Palm Oil and Soybean Oil System

A third natural lipid system was composed of PO/SO. Five different SFC, 3, 7, 9, 11, and 16 %, were tested for their elastic modulus. The resulting strain from micromanipulation of droplets and model projections can be seen in Fig. 7a. With the experimental parameters of 25 μm radii and interfacial tension of 6.23 mN/m inserted into the equation, the model predicts the correct trend but not the correct magnitude for PO/SO oil droplets undergoing coalescence. The model and experimental strains are statistically similar only at the highest log G' where droplets undergo total stability.

The model projections for the PO/SO elastic moduli experiment are comparable to the AMF system. Both fats resulted in larger values of elastic moduli than the other lipid systems. The model expected almost no coalescence to occur for all four AMF elastic moduli and the four highest elastic moduli of the PO/SO system, but experimentally, droplets underwent a wide degree of strain. Differences between the predicted and experimental strain may be due the arrangement of the crystalline fat structure within these oil droplets.

For the droplet radius experiment, five different sizes of droplets composed of PO/SO were investigated. In Fig. 7b, the model expects very low strain values to be seen for all droplet radii. At the largest droplet size, the model and experimental strains appear to coincide but are not statistically similar. Otherwise, the experimental strains are much higher than the model expected. The model does

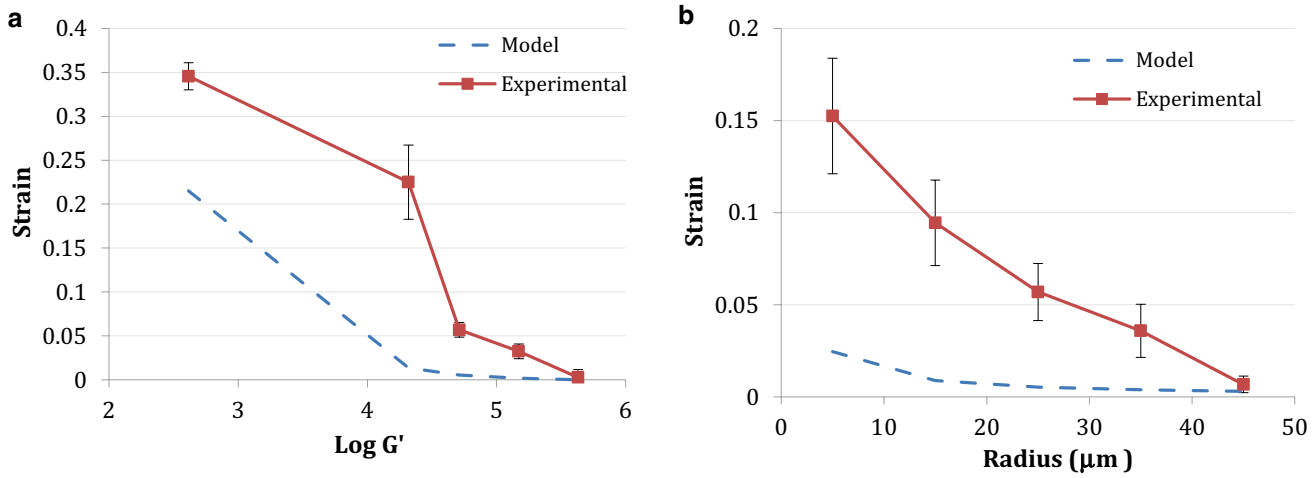

Fig. 7 Experimental and model strain values for palm oil and soybean oil (PO/SO) droplets at **a** five different elastic moduli **b** five different radii

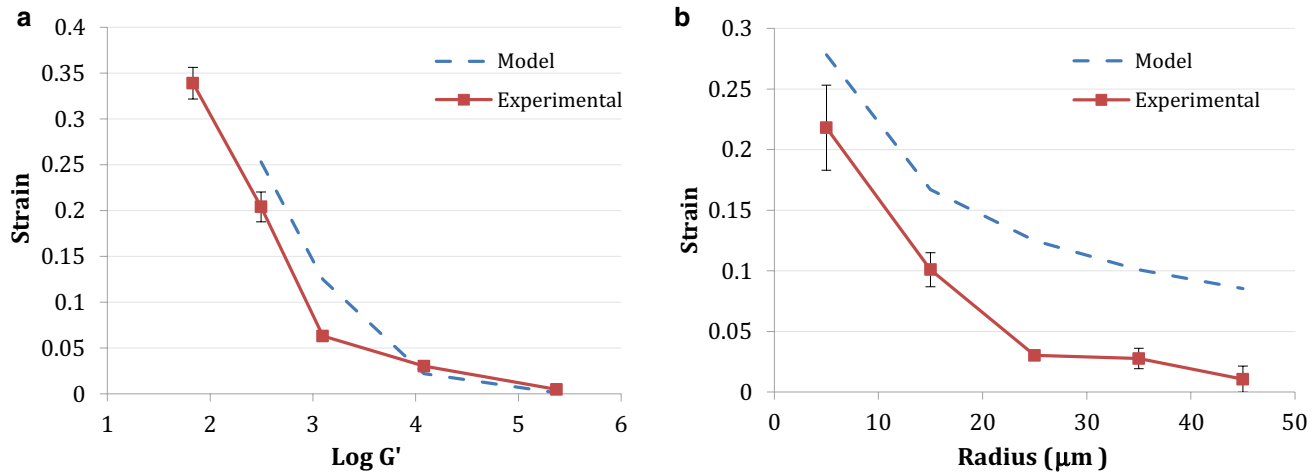

Fig. 8 Experimental and model strain values for coconut stearin and soybean oil (CS/SO) droplets at **a** five different elastic moduli **b** five different radii

not predict a large range in strain to be observed under the experimental parameters. Such findings mimic the droplet diameter experiment performed using AMF as the oil phase.

Coconut Stearin and Soybean Oil System

The last system involved mixtures of coconut stearin and soybean oil composing the oil phase. Once again model and experimental strains are compared in Fig. 8a. At the three lowest log G' values, the model underpredicts strain. The model appears to fit the experimental data at the two highest log G' values; however, only 30 % SFC led to statistically similar strains.

Micromanipulating different sizes of CO/SO droplets led to the model consistently predicting higher strains than experimentally observed in Fig. 8b. It appears that the model expected all five droplet radii tested to result in higher degrees of coalescence. A consistent overestimation of strain was also seen in the droplet radius experiment using PKO/SO. The PKO/SO and CS/SO systems used had lower log G' values for the droplet radius experiment than the two other natural fat systems. Accordingly, in both the PKO/SO and CS/SO experiments the model predicted higher strain than observed. The AMF and PO/SO systems had higher log G' values for the droplet radius experiment and the model expected lower strains to be seen. In all cases, droplets were 50 μm in size and interfacial tensions

were measured at 6.76 and 6.23 mN/m for systems using AMF and soybean oil, respectively. The model and experimental strain were never statistically similar in any droplet radius experiment performed on the four natural fat systems.

Conclusion

Micromanipulation techniques were used to investigate the coalescence behavior of droplets composed of different oils. Increasing the SFC of the oil phase led to higher G' values. For all fat systems, a larger G' led to coalescence being halted earlier, until total stability was reached. This is due to the internal rigidity of the droplets hindering the energetic drive to lower the total interfacial area via full coalescence. An inverse relationship was seen for droplet size and strain. The smaller the droplet radii became, the larger strain a pair underwent for all lipids used. For these experimental conditions, the expected trend of increasing the interfacial tension yielding an increase in strain for tristearin/triolein or AMF droplets was not observed. The energy balance model most closely predicted strains for elastic modulus experiments with the lipid phase composed of tristearin/triolein, PKO/SO, and CS/SO systems. It was seen that fat systems that obtained higher G' values, like AMF and PO/SO, did not fit the model. The model failed to predict experimental trends seen in all droplet radii experiments.

Acknowledgments This project was supported by [National Research Initiative or Agriculture and Food Research Initiative] Grant No 2014-67017-21652 from the USDA National Institute of Food And Agriculture, Nutrients and health, improving food quality—A1361.

References

1. Walstra P (2003) Changes in dispersity. Physical chemistry of foods. Marcel Dekker, New York
2. McClements DJ (2007) Critical review of techniques and methodologies for characterization of emulsion stability. Crit Rev Food Sci Nutr 47:611–649
3. Fredrick E, Walstra P, Dewettinck K (2010) Factors governing partial coalescence in oil-in-water emulsions. Adv Colloid Interface Sci 153(1):30–42
4. Giermanska J, Thivilliers F, Backov R, Schmitt V, Drelon N, Leal-Calderon F (2007) Gelling of oil-in-water emulsions comprising crystallized droplets. Langmuir ACS J Surf Colloids 23(9):4792–4799
5. Giermanska-Kahn J, Laine V, Arditty S, Schmitt V, Leal-Calderon F (2005) Particle-stabilized emulsions comprised of solid droplets. Langmuir ACS J Surf Colloids 21(10):4316–4323
6. Pawar A, Caggioni M, Ergun R, Hartel R, Spicer P (2011) Arrested coalescence in Pickering emulsions. Soft Matter 7(17):7710–7716
7. Pawar A, Caggioni M, Hartel R, Spicer P (2012) Arrested coalescence of viscoelastic droplets with internal microstructure. Faraday Discuss 158:341–350
8. Binks B (2002) Particles as surfactants—similarities and differences. Curr Opin Colloid Interface Sci 7(1):21–41
9. Van Boekel MAJS, Walstra P (1981) Stability of oil-in-water emulsions with crystals in the disperse phase. Colloids Surf 3(2):109–118
10. Boode K, Walstra P (1993) Partial coalescence in oil-in-water emulsions 1. Nature of the aggregation. Colloids Surf A 81:121–137
11. Darling D (1982) Recent advances in the destabilization of dairy emulsions. J Dairy Res 49(4):695–712
12. Fuller G, Considine T, Golding M, Matia-Merino L, Macgibbon A (2015) Aggregation behavior of partially crystalline oil-in-water emulsions: part II—effect of solid fat content and interfacial film composition on quiescent and shear stability. Food Hydrocoll 51:23–32
13. Fuller G, Considine T, Golding M, Matia-Merino L, Macgibbon A, Gillies G (2015) Aggregation behavior of partially crystalline oil-in-water emulsions: part I—characterization under steady shear. Food Hydrocoll 43:521–528
14. Moens K, Masum A, Dewettinck K (2016) Tempering of dairy emulsions: partial coalescence and whipping properties. Int Dairy J 56:92–100
15. Munk M, Andersen M (2015) Partial coalescence in emulsions: the impact of solid fat content and fatty acid composition. Eur J Lipid Sci Technol 117(10):1627–1635
16. Munk M, Marangoni A, Ludvigsen H, Norn V, Knudsen J, Risbo J, Ipsen R, Andersen M (2013) Stability of whippable oil-in-water emulsions: effect of monoglycerides on crystallization of palm kernel oil. Food Res Int 54(2):1738–1745
17. Thivilliers-Arvis F, Laurichesse E, Schmitt V, Leal-Calderon F (2010) Shear-induced instabilities in oil-in-water emulsions comprising partially crystallized droplets. Langmuir ACS J Surf Colloids 26(22):16782–16790
18. Goff H (1997) Instability and partial coalescence in whippable dairy emulsions. J Dairy Sci 80(10):2620–2630
19. Anderson M, Andrews AT (1986) The development of structure in whipped cream. Food Microstruct 5(2):277–285
20. Shiinoki Y, Noda M (1986) Microstructure and rheological behavior of whipping cream. J Texture Stud 17(2):189–204
21. Needs EC, Huitson A (1991) The contribution of milk serum proteins to the development of whipped cream structure. Food Struct 10(4):353–360
22. Stanley DW, Goff HD, Smith AK (1996) Texture-structure relationships in foamed dairy emulsions. Food Res Int 29(1):1–13
23. Lin PM, Leeder JG (1974) Mechanism of emulsifier action in an ice cream system. J Food Sci 39(1):108–111
24. Buchheim W, Barfod NM, Krog N (1985) Relation between microstructure, destabilization phenomena and rheological properties of whippable emulsions. Food Microstruct 4(2):221–232
25. Berger KG (1990) Ice cream. In: Friberg S, Larsson K (eds) Food emulsions, 2nd edn. Marcel Dekker Inc., New York
26. Goff HD, Hartel RW (2013) Ice Cream, 7th edn. Springer, New York